Electric Vehicle Induction Motor DSVM-DTC with Torque Ripple Minimization

Farid Khoucha, Khoudir Marouani, Abdelaziz Kheloui, Mohamed Benbouzid

Electric Vehicle Induction Motor DSVM-DTC with Torque Ripple Minimization

Farid Khoucha[1,2], Khoudir Marouani[2], Abdelaziz Kheloui[2], Mohamed El Hachemi Benbouzid[1]

Abstract–*This paper presents a sensorless DSVM-DTC of an induction motor that propels an electrical vehicle or a hybrid one. The drive uses an adaptive flux observer for speed estimation and a discrete space vector modulation direct torque control (DSVM-DTC) technique for torque and stator flux control. The adaptive flux observer uses a mechanical model to improve the behavior during speed transients. The estimated stator flux of the adaptive observer is used in the DSVM-DTC method to provide fast torque response combined with torque ripple free operation over the whole speed range. The sensorless drive system is capable of working from very low speed to high speed and exhibits good dynamic and steady-state performance. The combination of the adaptive observer and DSVM-DTC are quite effective in reducing the switching loss and torque ripples of the motor, as demonstrated in experimental results.*

Keywords*: Electric vehicle (EV), induction motor, Discrete Space Vector Modulation Direct Torque Control (DSVM-DTC), adaptive observer.*

I. Introduction

In the last decade, the increasing restrictions imposed on the exhaust emissions from internal combustion engines and the traffic limitations in the urban areas have given a strong impulse toward the development of electrical propulsion systems for automotive applications [1]. The major goal of electrical and hybrid vehicles is the reduction of global emissions, which in turn leads to a decrease of fuel resources exploitation.

The major components of an electric vehicle system are motor, controller, power source; charger and drive train. The majority of electric vehicles (EV) developed so far are based on dc machines, induction machines or permanent magnet machines. The disadvantages of dc machines forced the EV developers to look into various types of ac machines.

The power density of permanent magnet machines together with the high cost of permanent magnets makes these machines less attractive for EV applications. The maintenance-free and low-cost induction machines became a good attractive alternative to many developers. However, high-speed operation of induction machines is only possible with a penalty in size and weight. Three-phase squirrel cage-rotor induction motors are best suited to electric vehicle drive applications thanks to its well-known advantage of simple construction, reliability, ruggedness, and low cost [2].

Induction motor drives control techniques are well treated in the literature. The most popular is the so-called vector control technique that is now used for high impact automotive applications. In this case, the torque control is extended to transient state and allows better dynamic performances. Among these techniques, DTC appears to be very convenient for EV applications [3-4].

The DTC has the advantages of simplicity; it does not require speed or position encoders and uses voltage and current measurements only to estimate flux, torque. It also has a faster dynamic response since it does not require any current regulation, coordinates transformation and insensitivity to motor parameters except the stator winding resistance [5]. The input of the motor controller is the reference speed, which is directly applied by conductor from the pedal of the vehicle.

One of the disadvantages of conventional DTC is high switching loss and torque ripple because of the use of hysteresis band and the small number of applicable voltage vectors [6]. Several techniques have been developed to minimize switching loss and reducing the torque ripple [7]. One of them is duty ratio control method. In duty ratio control, a selected output voltage vector is applied for a portion of one sampling period, and a zero voltage vector is applied for the rest of the period. The pulse duration of output voltage vector is determined by the torque-ripple minimum condition. These improvements can greatly reduce the torque ripple, but they increase the complexity of DTC algorithm.

An alternative method to reduce the ripples is based on space vector modulation (SVM) technique [8-9]. At each cycle period, a preview technique is used to obtain the voltage space vector required to exactly compensate the flux and torque errors. The required voltage space vector can be synthesized using SVM technique.

SVM-DTC is significantly improved [10]. However, it requires calculating several complicate equations online, and it depends on more machine parameters. In [11] is presented a new DTC scheme using discrete space vector modulation (DSVM) technique. It is a control system able to generate a number of voltage vectors higher than that used in conventional DTC scheme. The increased number of voltage vectors allows the definition of more accurate switching tables. The DSVM-DTC achieves a sensible reduction of torque ripple, without increasing the DTC algorithm complexity.

II. Flux and Speed Estimation

II.1 Induction Motor Flux Observer

In the stationary reference frame fixed on stator, the dynamic behavior of induction motor can be described by the following model.

$$\begin{cases} \dot{x} = Ax + Bu \\ y = Cx \end{cases} \tag{1}$$

Where

$$x = \begin{bmatrix} i_{s\alpha} & i_{s\beta} & \varphi_{r\alpha} & \varphi_{r\beta} \end{bmatrix}^t$$

$$u = \begin{bmatrix} v_{s\alpha} & v_{s\beta} \end{bmatrix}^t$$

$$y = \begin{bmatrix} i_{s\alpha} & i_{s\beta} \end{bmatrix}^t$$

$$A = \begin{bmatrix} -\frac{1}{\sigma}\left(\frac{1-\sigma}{T_r}+\frac{1}{T_S}\right) & 0 & \frac{M}{\sigma L_r L_S T_r} & \frac{M}{\sigma L_r L_S}\omega_r \\ 0 & -\frac{1}{\sigma}\left(\frac{1-\sigma}{T_r}+\frac{1}{T_S}\right) & -\frac{M}{\sigma L_r L_S}\omega_r & \frac{M}{\sigma L_r L_S T_r} \\ \frac{L_m}{T_r} & 0 & -\frac{1}{T_r} & -\omega_r \\ 0 & \frac{L_m}{T_r} & \omega_r & -\frac{1}{T_r} \end{bmatrix}$$

$$B = \begin{bmatrix} \frac{1}{\sigma L_r} & 0 \\ 0 & \frac{1}{\sigma L_r} \\ 0 & 0 \\ 0 & 0 \end{bmatrix}$$

$$C = \begin{bmatrix} 1 & 0 & 0 & 0 \\ 0 & 1 & 0 & 0 \end{bmatrix}$$

With R_s et R_r the stator and rotor resistances, L_s et L_r the stator and rotor inductances, M the mutual inductance, and σ the leakage coefficient.

A state observer that provides rotor flux estimates is given by

$$\dot{\hat{x}}_S = A\hat{x} + BU + K\left(\hat{i}_S - i_S\right) \tag{2}$$

The symbol ^ denotes an estimated quantity. K is a gain matrix, which is used to suitably locate the observer poles.

II.2 Adaptive Flux Observer for Speed Estimation

By adding an adaptive scheme for estimating the rotor speed to the observer, both states unknown parameters can be estimated simultaneously. The adaptive scheme is derived using the Lyapunov theory [12]. From (1) and (2) the rotor flux and stator current estimation error is given by

$$\frac{de}{dt} = \left(A + KC\right)e + \Delta A x \tag{3}$$

Where $e = x - \hat{x}$

$$\Delta A = A - \hat{A} = \begin{bmatrix} -\Delta\omega_r J & 0 \\ 0 & 0 \end{bmatrix}$$

$$\Delta\omega_r = \omega_r - \hat{\omega}_r$$

$$J = \begin{bmatrix} 0 & -1 \\ 1 & 0 \end{bmatrix}$$

The Lyapunov candidate function V is defined as

$$V = e_n^T e_n + \left(\hat{\omega}_r - \omega_r\right)^2 / \lambda \tag{4}$$

where λ a is positive constant and

$$e_n = \begin{bmatrix} i_S - \hat{i}_S & \varphi_r - \hat{\varphi}_r \end{bmatrix}^T = \begin{bmatrix} e_{is} & e_{\varphi r} \end{bmatrix} = \Gamma e$$

with Γ a non-singular matrix.

For the derivation of the adaptive mechanism the unknown parameter is considered constant. The time derivative of V becomes

$$\dot{V} = e_n^T \left\{ \left[\Gamma\left(A+KC\right)\Gamma^{-1}\right]^T + \left[\Gamma\left(A+KC\right)\right]\Gamma^{-1} \right\} e_n + \hat{x}^T \Delta A^T \Gamma^T e_n + e_n^T \Gamma \Delta A \hat{x} - 2\Delta\omega_r \frac{d\hat{\omega}_r}{dt}/\lambda \tag{5}$$

The adaptive scheme for speed estimation is then given by

$$\hat{\omega}_r = K_{I\omega}\int\left[\varphi_{s\beta}e_{is\alpha} - \varphi_{s\alpha}e_{is\beta}\right]dt \qquad (6)$$

where $K_{I\omega}$ a positive constant.

The adaptive flux observer is stable according to the Lyapunov direct method if the observer gain is chosen such that the first term of (5) is negative semi-definite. This condition is fulfilled if the eigenvalues of $\Gamma(A + KC)\Gamma^{-1}$ have negative real parts. Since the eigenvalues of $\Gamma(A + KC)\Gamma^{-1}$ equal the eigenvalues of $(A + KC)$ the observer should have stable poles.

Although the adaptive scheme is derived under consideration of constant speed, in practice motor speed can change quickly. In order to improve the dynamic behavior of the speed estimation algorithm, a proportional term can be added [13]. Speed estimation becomes then

$$\hat{\omega}_r = K_{I\omega}\int\left[\varphi_{s\beta}e_{is\alpha} - \varphi_{s\alpha}e_{is\beta}\right]dt + K_{P\omega}\left[\varphi_{s\beta}e_{is\alpha} - \varphi_{s\alpha}e_{is\beta}\right] \qquad (7)$$

III. The Adopted Control Technique

The basic idea of DTC is to control flux and torque directly through closed-loop. Only when the amplitude and the phase angle of flux are estimated precisely, the real electromagnetic torque is calculated. So in order to get optimal steady state and dynamic response, the stator flux must be observed accurately, especially in low speed-range.

In principle the DTC selects one of the six voltage vectors and two zero voltage vectors generated by a VSI in order to keep stator flux and torque within the limits of two hysteresis bands. The right application of this principle allows a decoupled control of flux and torque without the need of coordinate transformation, PWM pulse generation and current regulators. However, the presence of hysteresis controllers leads to a variable switching frequency operation, in addition, the time discretization due to the digital implementation besides the limited number of available voltage vectors determine the presence of current and torque ripple.

Different methods have been presented which allow constant switching frequency operation. In general, they require control schemes which are more complex with respect to the basic DTC schemes.

With reference to current and torque ripple it has been verified that a large influence is exerted by the amplitude of flux and torque hysteresis bands, and the voltage vector selection criteria. It can be noted also that a given voltage vector has different effects on the drive behavior at high, medium and low speed. Taking these considerations into account, a good compromise has been obtained using different switching tables at high, medium and low speed [14]. In general, the determination of the switching tables is carried out on the basis of physical considerations concerning the effects determined by radial and tangential variation of the stator flux vector on torque and flux values. Although simple, this approach leads to unexpected torque variations in some particular operating conditions. The understanding of these phenomena requires a rigorous analytical approach taking the electromagnetic behavior of the machine into account.

A substantial reduction of current and torque ripple could be obtained using, at each cycle period, a preview technique in the calculation of the stator flux vector variation required to exactly compensate the flux and torque error. In order to apply this principle, the control system should be able to generate, at each sampling period, any voltage vector, this ideal behavior can be approximated using a control system able to generate a number of voltage vectors higher than that used in basic DTC scheme. These solutions are good for high power application, but are not acceptable for medium or low power application owing to the increased complexity of the power circuit.

In this paper a new control technique is introduced which allows the performance of DTC scheme in terms of flux, torque ripple and current distortion to be improved. These performances are achieved without increasing the complexity of the power circuit and the inverter switching frequency. The new control algorithm is based on discrete space vector modulation (DSVM) technique which uses prefixed time intervals within a cycle period. In this way and by using a two level inverter a higher number of voltage space vectors can synthesized with respect to those used in basic DTC technique.

III.1 The Basic DTC Technique

The basic model of DTC induction motor scheme is shown in Fig. 1. At each sample time, the two stator currents i_{sa} and i_{sb} and the DC bus voltage V_{dc} are sampled. Using the inverter voltage vector, the α-β components of the stator voltage space vector in the stationary reference frame are calculated as follows.

$$\begin{cases} V_{s\alpha} = \dfrac{2}{3}V_{dc}\left(S_a - \dfrac{S_b + S_c}{2}\right) \\ V_{s\beta} = \dfrac{1}{\sqrt{3}}V_{dc}\left(S_b - S_c\right) \end{cases} \qquad (8)$$

The α-β components of the stator current space vector are calculated using

$$\begin{cases} i_{s\alpha} = i_{sa} \\ i_{s\beta} = \dfrac{i_{sa} + 2i_{sc}}{\sqrt{3}} \end{cases} \qquad (9)$$

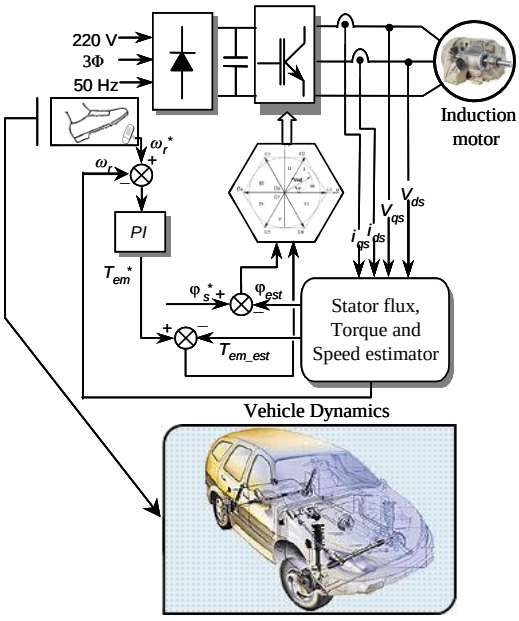

Fig.1. Basic direct torque control scheme.

The stator flux is a function of the rotor flux which is provides from the flux observer.

$$\begin{cases} \varphi_{s\alpha} = \sigma L_s i_{s\alpha} + \dfrac{M}{L_r}\varphi_{r\alpha} \\ \varphi_{s\beta} = \sigma L_s i_{s\beta} + \dfrac{M}{L_r}\varphi_{r\beta} \end{cases} \quad (10)$$

Then the magnitude of the stator flux and electromagnetic torque are calculated by

$$\begin{cases} |\varphi_s| = \sqrt{\varphi_{s\alpha}^2 + \varphi_{s\beta}^2} \\ T_e = \dfrac{3}{2} p \left(\varphi_{s\alpha} i_{s\beta} - \varphi_{s\beta} i_{s\alpha} \right) \end{cases} \quad (11)$$

where p is the number of pole pairs.

As shown in Fig. 2, a switching table is used for the inverter control such that the torque and flux errors are kept within the specified bands. The torque and flux errors are defined as

$$\begin{cases} \Delta T_e = T_e - \hat{T}_e \\ \Delta\varphi_s = \varphi_s - \hat{\varphi}_s \end{cases} \quad (12)$$

The inverter switching states are determined by the torque and flux errors according to the sector determined.

III.2 The DSVM-DTC

The DSVM technique uses a standard VSI and synthesizes a higher number of voltage vectors than those used in conventional DTC.

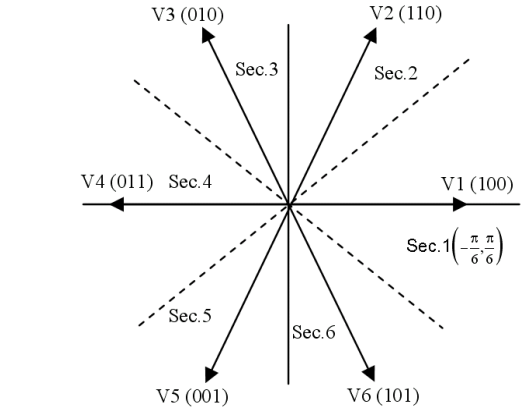

(a) Output voltage vectors.

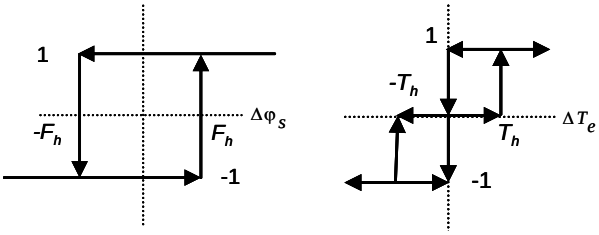

(b) Flux comparator. (c) Three-level torque comparator.

Fig.2. DTC definition of the voltage vectors and comparators.

Table 1. Classical DTC Switching table.

		Sector 6 (-90°, -30°)	Sector 5 (-30°, 30°)	Sector 4 (30°, 90°)	Sector 3 (90°, 150°)	Sector 2 (150°, 210)	Sector 1 (210°,270°)
Decrease Flux	Increase Torque	10 0	11 0	01 0	01 1	00 1	10 1
	Decrease Torque	01 1	00 1	10 1	10 0	11 0	01 0
Increase Flux	Increase Torque	11 0	01 0	01 1	00 1	10 1	10 0
	Decrease Torque	00 1	10 1	10 0	11 0	01 0	01 1

The implementation of the DSVM technique requires only a small increase of the computational time required by conventional DTC scheme.

In DSVM-DTC, one sampling period is divided into m equal time intervals. One of the VSI voltage vectors is applied in each of them. The number of voltage vectors, which can be generated, is directly related to m. The higher is m, the higher is the number of voltage vectors and the lower is the amplitude of the current and torque ripple, but more complex are the switching tables required. A good compromise between the errors compensation and the complexity of the switching tables is achieved by choosing $m = 3$ [15].

Using DSVM technique with three equal time intervals, 36 synthesized non-zero voltage vectors are

obtained. The stator flux is assumed to be in sector 1, then 19 voltage vectors can be used, as represented in Fig. 3. The black dots represent the ends of the synthesized voltage vectors. As an example, the label (556) denotes the voltage vector which is synthesized by using the standard VSI voltage vectors V5, V5 and V6, each one applied for one third of the sampling period, where Z denotes a zero voltage vector.

In order to fully utilize the available voltage vectors, one sector is subdivided into two parts, as shown in Fig. 3. As the torque reduction produced by a zero VSI voltage vector is much more evident at high speed, different voltage vectors are chosen for different speed range [16]. When the rotor speed is greater than one half of the synchronous speed, it belongs to the high speed range and when it is lower than one sixth, it is in the low speed range.

The DSVM-DTC switching table is summarized in Table 2, where C_φ and C_T are the flux and torque hysteresis controller outputs: C_φ has two levels ($C_\varphi = -1$ means that the amplitude of the stator flux exceeds the upper limit of its hysteresis band and should be reduced and $C_\varphi = +1$ means that the amplitude of the stator flux should be increased). C_T has five levels (a negative value of C_T means that the torque needs to decreased, and a positive value of C_T means that the torque needs to be increased. When C_T is −2 or +2, the torque is far away from its control value, and therefore needs a large and rapid change. When C_T is 0, the torque is equal or close to its control value, and should be kept unchanged.

For example, it is assumed that the rotor speed is in high speed range, and stator flux vector is in sector (1+). If C_φ is (−1) and C_T is (−2), the stator flux needs to be decreased and the torque needs to be largely decreased, so V15 (555) is chosen. If C_φ is (+1) and C_T is (−1), the stator flux needs to be increased and the torque needs to be slightly decreased. Considering that a zero VSI voltage vector can obviously reduce the torque in high speed range, V1 (2ZZ) is chosen.

Changing the sequence of the 3 voltage vectors applied to the 3 equal time intervals of one sampling period does not change the final synthesized voltage vector.

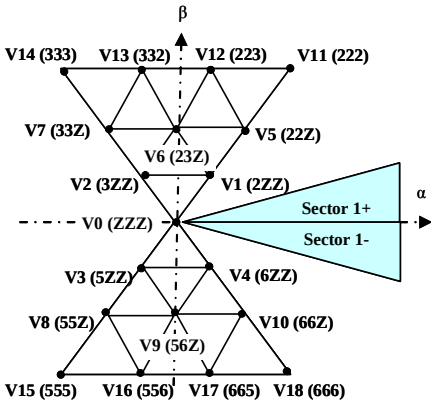

Fig. 3. Synthesized voltage vectors obtained using DSVM technique.

Table 2. DSVM-DTC switching table.

	C_φ	C_T				
		−2	−1	0	+1	+2
Low speed range	-1	555	5ZZ	ZZZ	3ZZ	333
	+1	666	6ZZ	ZZZ	2ZZ	222
Medium speed range	-1	555	ZZZ	3ZZ	33Z	333
	+1	666	ZZZ	2ZZ	22Z	222
High speed range Sector 1+	-1	555	3ZZ	33Z	333	333
	+1	666	2ZZ	23Z	223	222
High speed range Sector 1−	-1	555	3ZZ	23Z	332	333
	+1	666	2ZZ2	22Z	222	222

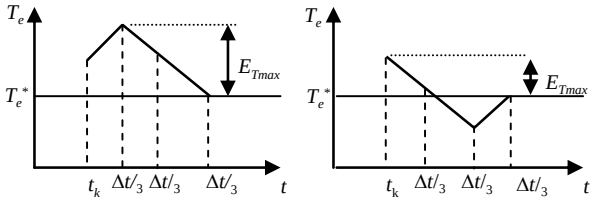

Fig. 4. Comparison of torque waveforms in one sampling period when C_T is −1: (a) Applying (3ZZ), (b) Applying (ZZ3).

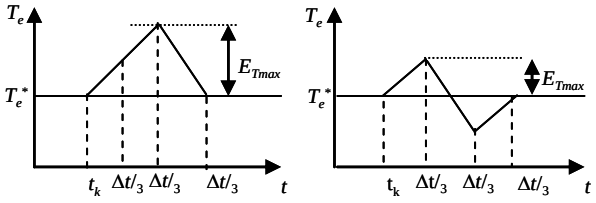

Fig. 5. Comparison of torque waveforms in one sampling period when C_T is 0: (a) Applying "3Z3", (b) Applying (33Z).

For example, (66Z), (6Z6) and (Z66) synthesize the same voltage vector V10. However, the sequence can greatly affect the torque ripple. If the 3 voltage vectors in one sampling period are applied in a proper sequence, the torque ripple can be reduced. It is assumed that the rotor speed is in high speed range, and the stator flux vector is in sector (1+). At time t_k, the beginning of a sampling period, C_φ is (−1) and C_T is (−1), which indicates that the actual torque value is greater than the reference value. The torque should be decreased. In this case, (3ZZ) is selected according to Fig. 3. Applying VSI voltage vector V3 can increase the torque, and a zero voltage vector causes a decrement. If V3 is firstly applied, the torque error will be enlarged. The torque waveform is shown in Fig. 4.a, where Δt is a sampling period time. In contrast, the torque waveform by applying (ZZ3) is shown in Fig. 4.b. Zero voltage vectors are firstly applied, causing the direct decrease of the torque. The torque error will not become larger. It can be seen from Fig. 4 that the maximum torque error E_{Tmax} produced by (ZZ3) is smaller than that produced by (3ZZ).

If C_T is (0) in the previous case, the actual torque value is equal or close to the reference torque value (33Z) is selected according to Table 2. The torque waveform is shown in Fig. 5. The torque increases to its maximum value, then decreases to the reference value. In order to minimize the torque ripple, the sequence of the 3 voltage vectors is changed, and (3Z3) is used. Applying (3Z3), the torque increases firstly, and decreases in the second time interval. In the third time interval the torque increases to its reference value, as shown in Fig. 5. The torque cannot reach the maximum value produced by (33Z). Therefore, the synthesized voltage vectors are selected from Table 2, but the sequence of their three components should be rearranged to reduce the torque ripple. When the torque needs to be decreased, the VSI voltage vectors which can decrease the torque should be firstly applied. Conversely, when the torque needs to be increased, the VSI voltage vectors which can increase the torque should be firstly applied. When the torque is equal or close to its reference value, the 3 VSI voltage vectors should be arranged in a symmetrical order.

IV. Experimental Results

The test bench used to validate the proposed control approach is made up of a 1.5-kW induction motor drive fed by a 2-level IGBT voltage source inverter whose ratings are given in the Appendix (Fig. 6).

The whole control algorithm (Adaptive speed and flux observer, DSVM-DTC algorithm and PI speed regulator) is implemented in a single fixed-point TMS320F240 DSP-based development board within less than 100 µs of time computing. The power components digital control signals are generated by the DSP-controller via PWM outputs. The control frequency is about 10 kHz. Voltage and current variables are measured by Hall-effect sensors and sampled at the same frequency. A mechanical speed sensor is mounted on the motor shaft only to allow comparison between estimated and measured speeds. It should be noted, as illustrated by Fig. 6, that the experimental setup was built to slightly emulate an EV.

A series of experimental results are depicted (Figs. 7 and 8), which represent the performances of the flux and speed adaptive observer under several conditions in association with the DSVM-DTC strategies. They prove the effectiveness of the adaptive observer in general and especially in association with the DSVM-DTC strategy. The whole control algorithm was implemented on a single DSP-controller board within a reasonable computing time, which leads to a good performance versus ease of implementation ratio.

V. Conclusion

This paper has presented two switching techniques for DTC of an induction motor drive that propels an electric vehicle associated to an adaptive speed observer.

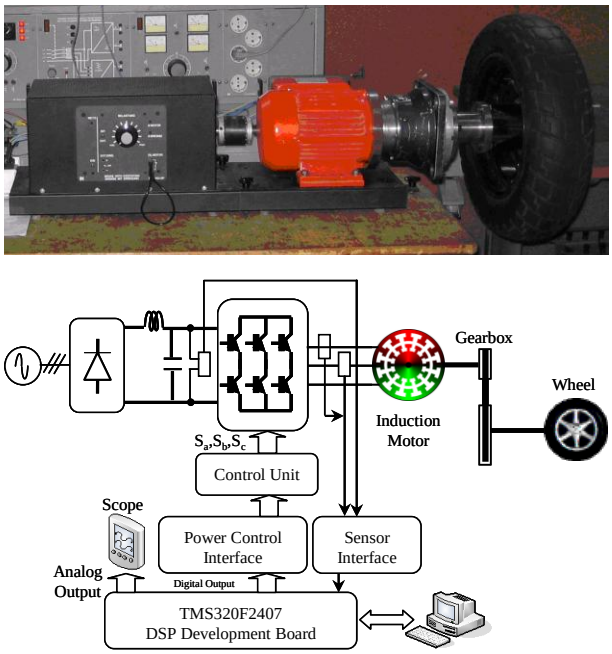

Fig. 6. The experimental setup.

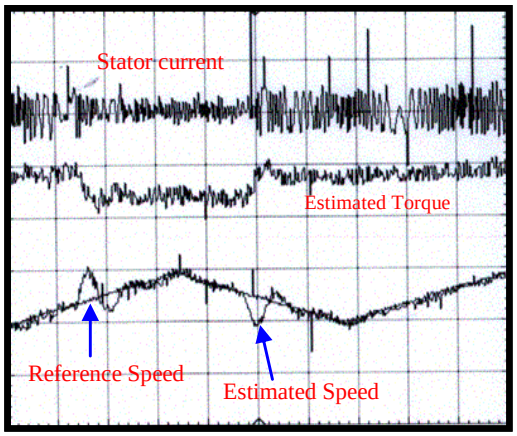

(a). Classical DTC.

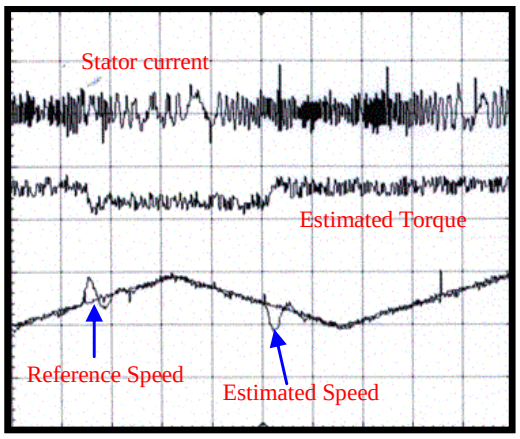

(b) DSVM-DTC.

Fig. 7. Experimental performances of the proposed control approach.

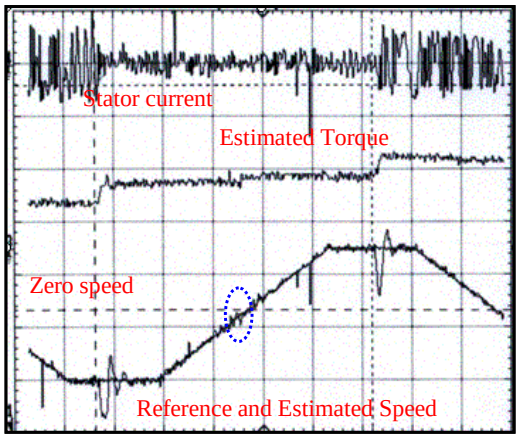

(a). Classical DTC.

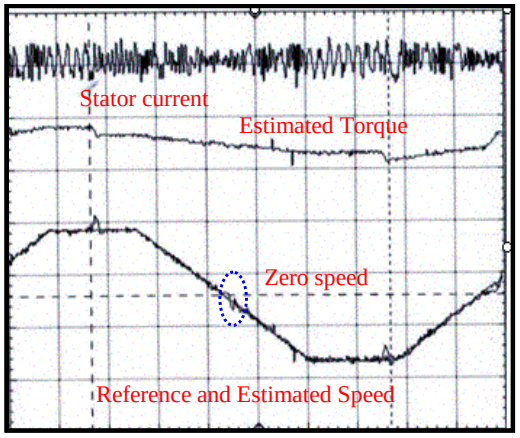

(b) DSVM-DTC.

Fig. 8. Experimental performances of the proposed control approach with speed reversal operation.

The adaptive flux observer uses a mechanical model to improve the speed estimation during speed transients. The estimated stator flux of the adaptive observer is used in the DTC to provide fast torque response combined with torque ripple free operation over the whole speed range .The presented experimental results have proved that the sensorless drive system is able to operate from very low to high speed and exhibits very good dynamics. Moreover, it has been shown that the DSVM-DTC strategy allows the torque, the rotor speed, and the current ripple to be reduced in comparison to the conventional DTC strategy.

Appendix

Rated Data of the Tested Induction Motor

1 kW, 50 Hz, 400/230 V, 3.4/5.9 A, 7 Nm, 2890 rpm
R_s = 4.67 Ω, R_r = 8 Ω, L_s = L_r = 0.347 H, M = 0.366 H
J = 0.06 kg.m², β = 0.042 Nm.sec

Reference

[1] C.C. Chan, "The state of the art of electric and hybrid vehicles," *Proceedings of the IEEE*, vol. 90, n°2, pp. 247-275, February 2002.

[2] M.E.H. Benbouzid et *al.*, Electric motor drive selection issues for HEV propulsion systems: A comparative study, *IEEE Trans. Vehicular Technology*, vol. 55, n°6, pp. 1756-1764, November 2006.

[3] J. Jung et *al.*, "A vector control schemes for ev induction motors with a series iron loss model," *IEEE Trans. Industrial Electronics*, vol. 45, n°4, pp. 617-624, August 1998.

[4] D.O. Neacsu et *al.*, "Comparative analysis of torque-controlled IM drives with applications in electric and hybrid vehicles vehicle," *IEEE Trans. Power Electronics*, vol. 16, n°2, pp. 240-247, March 2001.

[5] G.S. Buja et *al.*, "Direct torque control of PWM inverter-fed ac motors—A survey," *IEEE Trans. Industrial Electronics*, vol. 51, n°4, pp 744-757, August 2004.

[6] Y.S. Lai et *al.*, "Novel switching techniques for reducing the speed ripple of AC drives with direct torque control," *IEEE Trans. Industrial Electronics*, vol. 51, n°4, pp 768-775, August 2004.

[7] D. Telford et *al.*, "A novel torque-ripple reduction strategy for direct torque control," *IEEE Trans. Industrial Electronics*, vol. 48, n°4, pp 867-870, August 2001.

[8] T.G. Habetler et *al.*, "Direct torque control of induction machines using space vector modulation," *IEEE Trans. Industry Applications*, vol. 28, n°5, pp 1045-1053, September-October 1992.

[9] J. Kang et *al.*, "New direct torque control of induction motor for minimum torque ripple and constant switching frequency," *IEEE Trans. Industry Applications*, vol. 35, n°5, pp. 1076–1082, September-October 1999.

[10] T.G. Habetler et *al.*, "Control strategies for direct torque control using discrete pulse modulation," *IEEE Trans. Industry Applications*, vol. 27, n°5, pp. 893-901, September-October 1991.

[11] D. Casadei et *al.*, "Improvement of direct torque control performance by using a discrete SVM technique," in *Proceedings of IEEE PESC'98*, vol. 2, pp. 997-1003, May 1998.

[12] J. Maes et *al.*, "Speed-sensorless direct torque control of induction motors using an adaptive flux observer," *IEEE Trans. Industry Applications*, vol. 36, n°3, pp. 778-785, May-June 2000.

[13] H. Kubota et *al.*, "DSP-based adaptive flux observer of induction motor," *IEEE Trans. Industry Applications*, vol. 29, n°2, pp. 344-348, March-April 1993.

[14] S.H. Jeon et *al.*, "Flux observer with online tuning of stator and rotor resistances for induction motors," *IEEE Trans. Industrial Electronics*, vol. 49, n°3, pp. 653-664, June 2002.

[15] D. Casadei et *al.*, "Implementation of a direct control algorithm for induction motors based on discrete space vector modulation," *IEEE Trans. Power Electronics*, vol. 15, n°4, 769-777, July 2000.

[16] F. Khoucha et *al.*, "Experimental performance analysis of adaptive flux and speed observers for direct torque control of sensorless induction machine drives," in *Proceedings of IEEE PESC'04*, vol. 4, pp. 2678-2683, November 2004.

[1]University of Brest, EA 4325 LBMS, Rue de Kergoat, CS 93837, 29238 Brest Cedex 03, France (e-mail: m.benbouzid@ieee.org).
[2]Electrical Engineering Department, Polytechnic Military Academy, 16111 Algiers, Algeria.

Farid Khoucha was born in Khenchela, Algeria, in 1974. He received the B.Sc. and the M.Sc. degrees in Electrical Engineering, from the Polytechnic Military Academy, Algiers, Algeria, in 1998 and 2003 respectively. In 2000, he joined the Electrical Engineering Department of the Polytechnic Military Academy, Algiers, Algeria as a Teaching Assistant.

He is currently pursuing Ph.D. studies on electric and hybrid vehicle control and power management.

Khoudir Marouani was born in Constantine, Algeria, in 1972. He received the B.Sc. and the M.Sc. degrees in Electrical Engineering, from the Polytechnic Military Academy, Algiers, Algeria, in 1996 and 2000 respectively. In 2000, he joined the Electrical Engineering Department of the Polytechnic Military Academy, Algiers, Algeria as a Teaching Assistant.

He is currently pursuing Ph.D. studies. His main research interests include power electronics, electrical drives and active power filters.

Abdelaziz Kheloui received the M.Sc. degree in Electrical Engineering from the Ecole Nationale d'Ingénieurs et Techniciens of Algeria (ENITA), Algiers, Algeria in 1990 and the Ph.D. degree also in Electrical Engineering from the National Polytechnic Institute of Lorraine, Nancy, France in 1994. Since 1994 he has been an Assistant than an Associate Professor at the Electrical Engineering Department of the Polytechnic Military Academy, Algiers, Algeria.

His current research interests are control of electrical drives and power electronics.

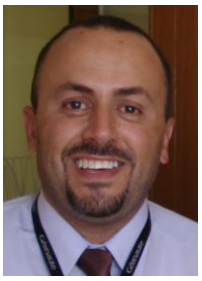

Mohamed El Hachemi Benbouzid was born in Batna, Algeria, in 1968. He received the B.Sc. degree in electrical engineering from the University of Batna, Batna, Algeria, in 1990, the M.Sc. and Ph.D. degrees in electrical and computer engineering from the National Polytechnic Institute of Grenoble, Grenoble, France, in 1991 and 1994, respectively, and the Habilitation à Diriger des Recherches degree from the University of Picardie "Jules Verne," Amiens, France, in 2000.

After receiving the Ph.D. degree, he joined the Professional Institute of Amiens, University of Picardie "Jules Verne," where he was an Associate Professor of electrical and computer engineering. In September 2004, he joined the IUT of Brest, University of Brest, Brest, France, as a Professor of electrical engineering. His main research interests and experience include analysis, design, and control of electric machines, variable-speed drives for traction and propulsion applications, and fault diagnosis of electric machines.

Prof. Benbouzid is a Senior Member of the IEEE Power Engineering, Industrial Electronics, Industry Applications, Power Electronics, and Vehicular Technology Societies. He is an Associate Editor of the IEEE TRANSACTIONS ON ENERGY CONVERSION, the IEEE TRANSACTIONS ON INDUSTRIAL ELECTRONICS, the IEEE TRANSACTIONS ON VEHICULAR TECHNOLOGY, and the IEEE/ASME TRANSACTIONS ON MECHATRONICS.